Cluster Spreads for Time-Variant Vehicular Channels

Zhinan Xu*, Mingming Gan*, Christoph F. Mecklenbräuker†, Thomas Zemen*,◇
*FTW (Telecommunications Research Center Vienna), Vienna, Austria
†Institute of Telecommunications, Vienna University of Technology, Vienna, Austria
◇ AIT Austrian Institute of Technology, Vienna, Austria
Contact: xu@ftw.at

***Abstract*—Cluster based channel models can be used to reduce the computational complexity. For vehicular communications, the environment changes rapidly due to the high velocities of the transmitter and receiver, resulting in fast changing cluster parameters. In this paper, we present an automatic cluster identification and tracking algorithm in order to consistently characterize the evolution of cluster parameters, e.g. delay and Doppler spreads. We apply the algorithm to a set of vehicular channel measurements. By analyzing the time-variant spreads of clusters, we find that the cluster associated with line-of-sight (LOS) components usually also consists of multipath components coming from several other objects, thus resulting in more dynamically changing spreads. Clusters at high Doppler shifts, stemming from big vehicle driving in the opposite direction, exhibit stable spreads. We apply the algorithm to a set of vehicular channel measurements and provide the fitting parameters.**

I. Introduction

In order to design reliable vehicular communication systems, we need a comprehensive understanding of the true propagation conditions of vehicular radio channels. As shown by vehicular radio channel measurements at 5 GHz, the impulse response of vehicular channels is mainly composed of: line-of-sight (LOS), deterministic scattering, and diffuse scattering. The LOS component contains a strong power gain if there exists a direct connection between the transmitter (Tx) and the receiver (Rx). The gain may drop due to shadowing effects and obstruction through interacting objects. In these cases, other multipath components (MPCs) become more relevant.

Furthermore, the statistical properties of the vehicular channel change over time and therefore the channel is non-stationary [1]. For this reason, the commonly used tap delay line channel model [2] is not suitable for vehicular communications. In order to obtain realistic simulation results, we need a non-stationary channel model that resembles the true propagation conditions. Because of that, the vehicular non-stationary channel model, named geometry-based stochastic channel model (GSCM), is developed for highway [3] and intersections [4], where the scatterers causing the MPCs are randomly placed according to a spatial distribution. However, the complexity of a GSCM is high due to the summation of a large number of complex exponentials (see (14) in [4]).

We are interested in a cluster based vehicular channel model resulting in a much lower computational complexity. The reduction of complexity comes in two-fold: 1) In this work, we model only the relevant MPCs above a certain power level. The MPCs with weak power contribution will be masked by the noise, thus they can neither be exploited by the Rx nor have an impact on the Rx performance. 2) Moreover, we further reduce the complexity by clustering the MPCs exhibiting similar properties.

As indicated in [5], the delay and Doppler spreads have a strong impact on the Rx performance, which makes channel modelling in these two domains more important. Therefore, we perform the clustering algorithm using a delay-Doppler power spectrum estimate in form of the local scattering function [1]. MPCs having similar delay and Doppler shift will form a cluster. In order to develop an accurate cluster based channel model, the knowledge of each cluster's energy concentration in these two domains is of great importance. In this paper, we analyze delay and Doppler spreads of the identified clusters. Thanks to the tracking algorithm, we are able to investigate also their corresponding evolution in time.

Contributions of this paper are:

- We propose to use the density-based scan algorithm with noise (DBSCAN) to group the MPCs into clusters.
- On top of DBSCAN, we use a simple yet efficient tracking algorithm to identify the time-variant cluster parameters.
- We analyze the cluster's delay and Doppler spreads. The clusters formed by different MPCs exhibit distinct dynamics over time.
- We apply the algorithm to a set of vehicular channel measurements where the LOS between the Tx and Rx was intermittently obstructed. We fit the distributions of the delay and Doppler spreads and provide the fitting parameters for all the measurements.

II. The Cluster's Joint Spread

We consider $L(t)$ MPCs at time instant t. Every single MPC l is associated with power $P_l(t)$ and parameter vector $\mathbf{x}_l(t) = [\tau_l(t), \nu_l(t)]^{\mathrm{T}}$ containing the delay and Doppler, where $l \in [1, \ldots, L]$. Denoting the set of MPCs indices belonging to cluster i at time instant t by $\mathcal{I}_i(t)$, the joint cluster spread is given by

$$\mathbf{C}_i(t) = \frac{\sum_{l\in\mathcal{I}_i(t)} P_l(t)\big(\mathbf{x}_l(t) - \boldsymbol{\mu}_i(t)\big)\big(\mathbf{x}_l(t) - \boldsymbol{\mu}_i(t)\big)^{\mathrm{T}}}{\sum_{l\in\mathcal{I}_i(t)} P_l(t)}, \tag{1}$$

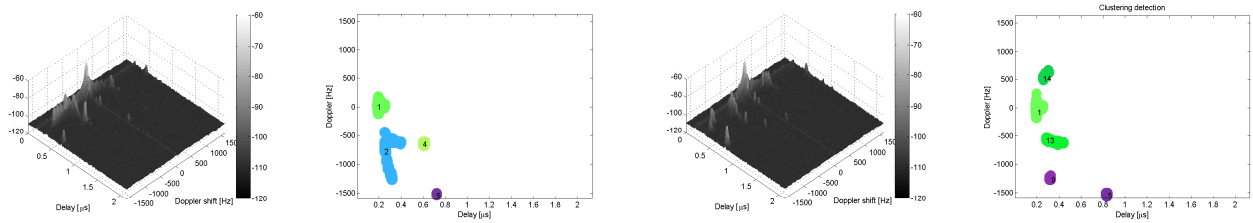

(a) Local scattering function at t_0 (b) Cluster identification t_0 (c) Local scattering function at t_1 (d) Cluster identification t_1

Fig. 1. Local scattering function and identified clusters at two different time instants t_0 and t_1

where the position of the weighted cluster centroid $\boldsymbol{\mu}_i(t)$ is defined as

$$\boldsymbol{\mu}_i(t) = [\tau_i(t), \nu_i(t)]^{\mathrm{T}} \tag{2}$$

$$= \frac{1}{\sum_{l\in\mathcal{I}_i(t)} P_l(t)} \begin{bmatrix} \sum_{l\in\mathcal{I}_i(t)} P_l(t)\tau_l(t) \\ \sum_{l\in\mathcal{I}_i(t)} P_l(t)\nu_l(t) \end{bmatrix}. \tag{3}$$

The 2×2 covariance matrix $\mathbf{C}_i(t)$ is symmetric where its main diagonal entries represent the root mean square (RMS) cluster spread in the delay and Doppler domain and off-diagonal entries represent the respective correlation between these spreads. The advantage of using a covariance matrix is that it provides a natural way of fusing multiple characteristics without normalization. The noise associated with MPCs are greatly filtered out by averaging over each individual covariance matrix.

III. Cluster Identification and Tracking

The vehicular environment changes rapidly due to the high velocities of the Tx and Rx. This also results in fast changing cluster parameters. In order to consistently characterize the evolution of cluster parameters over time, we introduce our cluster identification and tracking algorithm in this section.

A. Data Preprocessing

We are only interested in relevant MPCs above a certain power level. At the first step, we need to identify them from the channel impulse response, employing the power threshold criterion [6], where two power thresholds are used. A path exists if both of the following two criteria are satisfied:

- the power of the MPC is m_{th}dB above the noise floor.
- the power of the MPC is not more than n_{th}dB below the highest detected peak.

In this work, we choose $m_{\text{th}} = 10$ and $n_{\text{th}} = 25$. The MPCs which do not satisfy the above criteria are set to zero.

B. Cluster Identification

In order to identify the clusters formed by the relevant MPCs, the DBSCAN algorithm [7] is used, which is a density-based clustering algorithm to discover clusters of arbitrary shape. DBSCAN does not require one to specify the number of clusters in the data a priori, as opposed to the KPowerMeans [8]. DBSCAN requires only two input parameters, i.e. neighborhood radius *eps* and the minimum number of objects in a neighborhood *minPts*. The user can determine an appropriate value for it. The DBSCAN algorithm finds clusters with the following steps.

- It starts with an arbitrary starting point and finds all the neighbor points within distance *eps* of the starting point. A cluster will be formed if the number of neighbors is greater than or equal to *minPts*. The starting point and its neighbors are included in this cluster and the starting point is marked as visited.
- The algorithm then repeats the evaluation process for all the neighbors recursively. If the number of neighbors is less than *minPts*, the point is marked as noise.
- If a cluster is fully expanded (all reachable points are visited) then the algorithm proceeds with the remaining unvisited points in the dataset.

In this work, we use *minPts*=2 and *eps*=8.

C. Cluster Tracking

The purpose of tracking is to capture the evolution of cluster parameters, e.g. centroid movement, time-variant cluster spreads. The idea of the algorithm is based on a distance measure of clusters' centroids, named multipath component distance [9]. A number of $N(t)$ cluster centroids $\boldsymbol{\mu}_i(t)$ are detected at time instant t, where $i \in \{1, \ldots, N(t)\}$. We denote by t the current snapshot and by $t-1$ the previous snapshot. The algorithm is given as follows.

- It calculates the MCD between any old (at time $t-1$) and any new centroids (at time t).
- If the distance between a new centroid and its closest old centroid is larger than a predefined threshold, the new centroid is regarded as a newly detected centroid.
- For each old centroid, check the number of new centroids within the threshold.
  - If the number $= 1$, the old centroid is moved.
  - If the number > 1, the old centroid splits. The closest new one is regarded as old moved centroid. All other are treated as new centroids.

Fig. 1 shows the local scattering function and the identified clusters of an exemplary vehicular channel measurement in the delay-Doppler domain at two different time instants. Each cluster is colored according to the cluster ID given by the tracking algorithm. At time instant t_0, four clusters are detected. Cluster 1 corresponds to the LOS component, which exists in both time instants. Cluster 5 stemming from the vehicle in the opposite direction, appears also in both time

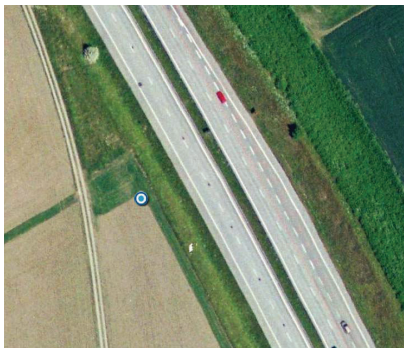

Fig. 2. : Map of measurement environment near the city of Lund (Copyright: Google Earth, http://earth.google.com/)

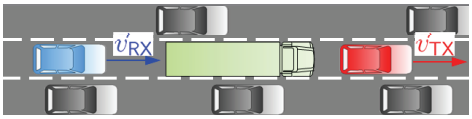

Fig. 3. Measurement schematic

instants. However the postion of Cluster 5 is changed due to the movements of the vehicles. Cluster 2 disappears and splits into several clusters at t_1.

IV. Measurement Data

We use the measurements collected in the DRIVEWAY'09 V2V measurement campaign in Lund, Sweden [10]. The measurements are collected using a center frequency of 5.6 GHz and a bandwidth of 240 MHz. There are 769 frequency samples with a frequency separation of 312 kHz. A measurement run covers a duration of 10 s at a repetition time of 307.2 μs, resulting in a total of 32500 snapshots. The data collected in the DRIVEWAY'09 campaign covers a wide range of safety critical scenarios, in this paper we focus on the highway scenario with obstructed LOS, in which the Tx and Rx are driving in the same direction at around 120km/h. The highway segment selected for experiments is shown in Fig. 2, which consists of three lanes in each direction and vegetation in the vicinity of the highway. There are big trucks which are intermittently obstructing the LOS between TX and RX. The traffic pattern during the measurements is similar to Fig. 3.

V. Simulation Results

We have 12 measurement runs performed in the highway scenario with obstructed LOS. In this section we will demonstrate the results and fitting of the empirical distributions for one measurement. Then, we perform the same analysis for the whole data set and provide the fitting parameters.

For cluster i, we extract the RMS values of delay spread $S_i^\tau(t)$ and Doppler spread $S_i^\nu(t)$ from the $\mathbf{C}_i(t)$, where

$$S_i^\tau(t) = \sqrt{\mathbf{C}_{i[1,1]}(t)} \text{ and } S_i^\nu(t) = \sqrt{\mathbf{C}_{i[2,2]}(t)}. \quad (4)$$

In order to analyze the time-variant cluster spreads, we plot in Fig. 4 the movement of cluster centroids during the entire

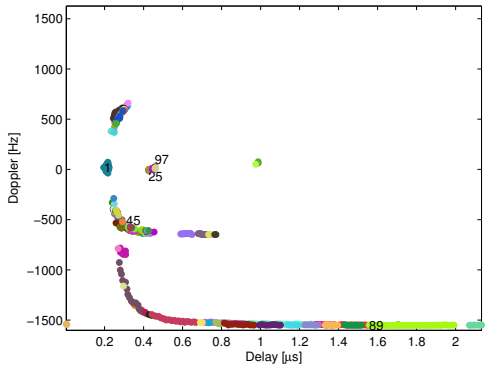

Fig. 4. Movement of cluster centroids in a 10 s measurement run. The centroids with the same color are from the same cluster.

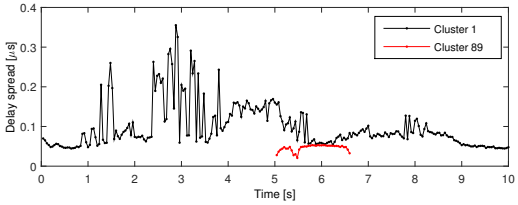

(a) Delay spread

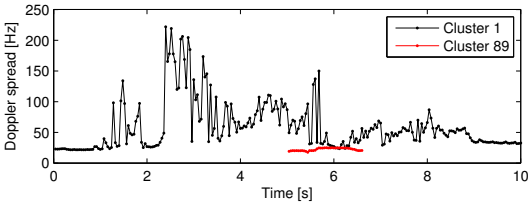

(b) Doppler spread

Fig. 5. Delay and Doppler spread of cluster 1 and culster 89 in their corresponding lifetime

10 s measurement run. We append the IDs of the clusters which have a lifetime longer than 1.2 s. Cluster 1 is related to the obstructed LOS component. We can observe that more clusters are detected at negative Doppler frequencies due to the existence of big trucks in the opposite lane behind the Tx and Rx vehicles.

In Fig. 5, we plot the delay and Doppler spreads of cluster 1 and 89 in their corresponding lifetime. Cluster 1 exists throughout the entire measurement run, while Cluster 89, stemming from the vehicle in the opposite direction, appears only from 5 s to 6.7 s. We can observe that the spread of cluster 1 changes rapidly in the time interval from 1 s to 6 s. This is due to the richness of MPCs that appear around the origin. From 1 s to 6 s, two big trucks traveling in the opposite direction are right in between the Tx and Rx. The MPCs due to the contribution of these scatterers locate very close to the position of the LOS component. The clustering algorithm will not separate them, thus resulting in a large delay and Doppler spreads of the merged cluster. On the other hand, the spreads of cluster 89 are relatively low due to the small size of the

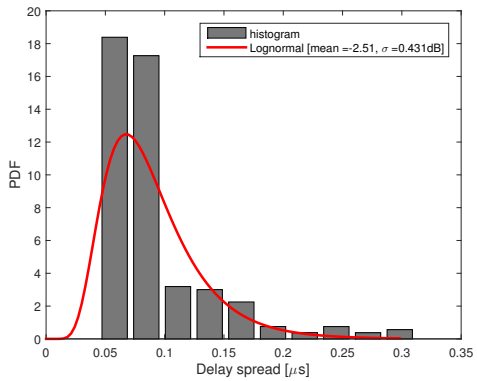

(a) Delay spread

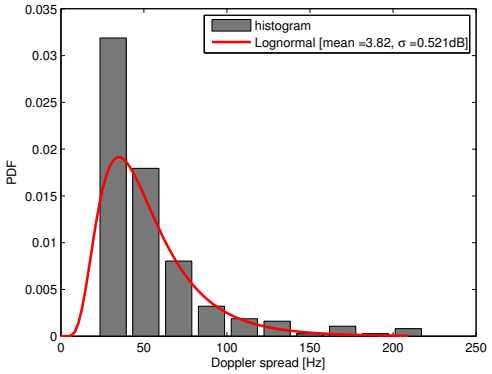

(b) Doppler spread

Fig. 6. Distribution of delay and Doppler spreads of cluster 1 (Cluster corresponding to the LOS).

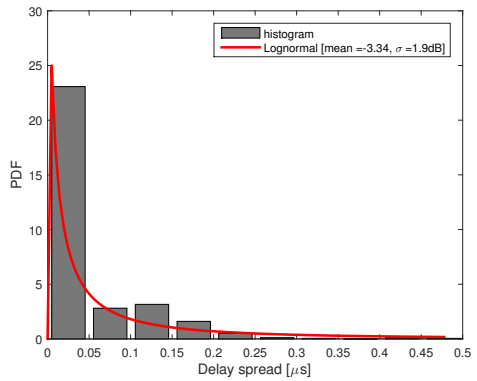

(a) Delay spread

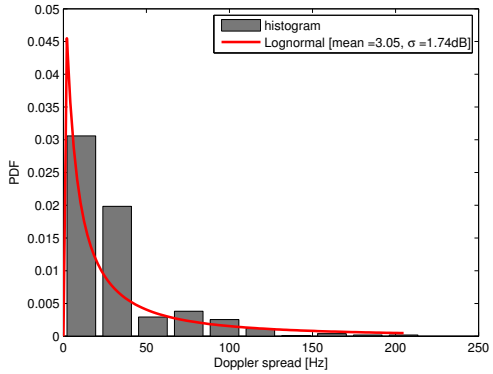

(b) Doppler spread

Fig. 7. Distribution of delay and Doppler spreads of other cluster.

cluster and remain almost unchanged over the lifetime.

The cluster corresponding to LOS exhibits different characteristics from the other clusters. hence we will analyze the distribution of the LOS cluster and the rest of clusters separately to obtain a better fit.

The distribution of delay and Doppler spreads of cluster 1 (the cluster corresponding to the LOS component) is presented in Fig. 6(a) and Fig. 6(b). The lognormal pdf is fitted to both spreads. For the delay spread, a mean of 2.52 and standard deviation of 0.43 gives a reasonable fit to the histogram. For the Doppler spread, a lognormal with a mean of 3.82 and a standard deviation of 0.52 fits our empirical results.

The distribution of delay and Doppler spreads of the other clusters (except for cluster 1) is presented in Fig. 7(a) and Fig. 7(b). We can observe that these clusters have smaller spreads compared to cluster 1.

In order to find the relationship between delay spread and Doppler spread, Fig. 8 shows the scatter plot of the delay spread versus Doppler spread for LOS cluster and the other clusters respectively. We can observe that delay and Doppler spreads are correlated for the cluster associated with LOS. This indicates that the extension of the LOS cluster occurs in both domains simultaneously for the investigated measurement. Moreover, a least-squares linear regression line is

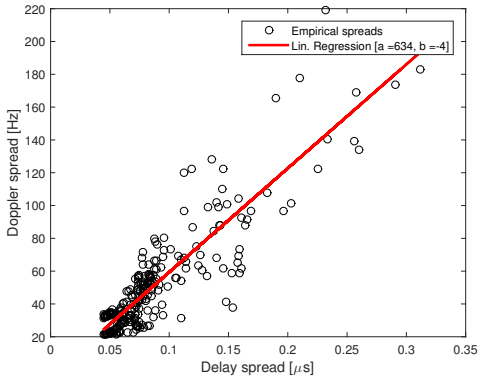

Fig. 8. Scatter plot of the delay spread versus Doppler spread for cluster 1 (corresponding to the LOS component) with a least-squares linear regression line.

superimposed on the scatter plot, which satisfies $S^{\nu} = aS^{\tau} + b$ with $a = 634$ and $b = -4$.

For the rest of the clusters, the delay and Doppler spreads concentrate more on small values, which can be seen in Fig. 9. Moreover, we observe a similar correlation as in Fig. 8.

We performed the same analysis for the whole set of measurements. Table I presents 1) the mean value and the standard deviation for lognormal distribution, and 2) the parameters

TABLE I
FITTING PARAMETERS FOR ALL 12 MEASUREMENT RUNS

Parameters	Cluster 1						Other clusters					
	Delay		Doppler		Delay/Doppler		Delay		Doppler		Delay/Doppler	
	mean	std	mean	std	a	b	mean	std	mean	std	a	b
Meas1	-2.51	0.43	3.82	0.52	633.52	-4.00	-3.34	1.90	3.05	1.74	429	7.37
Meas2	-2.15	0.30	3.50	0.27	199.05	10.65	-3.32	1.78	3.05	0.70	132	16.2
Meas3	-2.42	0.46	3.66	0.83	1085.62	-47.17	-3.36	1.87	3.09	1.34	426	7.48
Meas4	-2.99	0.28	3.29	0.17	32.85	25.50	-3.78	2.07	2.94	0.73	231	12.6
Meas5	-2.78	0.22	3.25	0.14	-51.57	29.29	-4.09	2.34	2.90	0.36	649	1.4
Meas6	-3.19	0.16	3.06	0.08	143.91	15.42	-3.31	0.17	3.07	0.18	377	8.08
Meas7	-2.55	0.41	3.66	0.39	480.16	1.36	-3.64	1.94	2.82	2.16	712	1.78
Meas8	-2.71	0.32	3.41	0.30	299.74	10.93	-3.52	1.86	3.08	1.12	665	0.525
Meas9	-3.02	0.19	3.27	0.14	-19.40	27.45	-3.87	2.18	2.90	0.70	207	12.5
Meas10	-3.01	0.22	3.34	0.12	86.53	24.00	-2.93	0.86	3.30	0.98	192	19.2
Meas11	-3.10	0.17	3.33	0.13	34.28	26.64	-3.47	0.87	2.93	0.87	131	15.8
Meas12	-2.66	0.23	3.25	0.13	111.80	18.00	-3.36	1.67	3.04	0.24	80.9	17.8

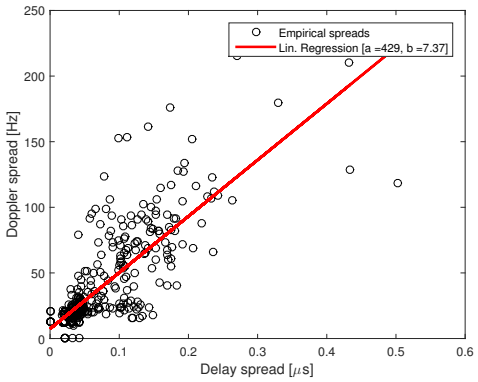

Fig. 9. Scatter plot of the delay spread versus Doppler spread for other clusters with a least-square linear regression line.

a and b for the linear regression line. These parameters are provided for delay and Doppler spreads for cluster 1 and the other clusters respectively. It is noteworthy that the relationship between delay and Doppler spreads vary significantly for different measurements. For measurements 5 and 9 where one strong LOS component exists, we may also have negative values for a occasionally, which suggests that the increase of the delay spread may result in a decrease of the Doppler spread.

VI. CONCLUSIONS

We presented an automatic cluster identification and tracking algorithm in order to consistently characterize the evolution of cluster delay and Doppler spreads. We applied the algorithm to a set of vehicular channel measurements where the LOS between the Tx and Rx was intermittently obstructed during the measurement. By analyzing the time-variant spreads of clusters, we found that the cluster associated with line-of-sight (LOS) components usually also consists of multipath components (MPCs) coming from several different scatterers, thus resulting in more dynamically changing spreads. Other clusters, stemming from a single scatterer, stay more stable in delay-Doppler domain. We fitted the distributions of the delay and Doppler spreads and provide the fitting parameters for all the measurements, which will be used for our follow-up research in developing an efficient yet accurate cluster-based vehicular channel model.

ACKNOWLEDGMENT

This work was performed in the FTW project Future ITS, a scientific cooperation co-funded by Kapsch TrafficCom AG and Vienna University of Technology.

REFERENCES

[1] L. Bernadó, T. Zemen, F. Tufvesson, A. F. Molisch, and C. F. Mecklenbräuker, "Delay and Doppler spreads of nonstationary vehicular channels for safety-relevant scenarios," *IEEE Trans. Veh. Technol.*, vol. 63, no. 1, pp. 82–93, Jan. 2014.

[2] G. Acosta-Marum and M. Ingram, "Six time- and frequency- selective empirical channel models for vehicular wireless LANs," *IEEE Veh. Technol. Mag.*, vol. 2, no. 4, pp. 4–11, Dec. 2007.

[3] J. Karedal, F. Tufvesson, N. Czink, A. Paier, C. Dumard, T. Zemen, C. F. Mecklenbräuker, and A. Molisch, "A geometry-based stochastic MIMO model for vehicle-to-vehicle communications," *IEEE Trans. Wirel. Commun.*, vol. 8, no. 7, pp. 3646–3657, Jul. 2009.

[4] Z. Xu, L. Bernadó, M. Gan, and M. Hofer, "Relaying for IEEE 802.11 p at Road Intersection Using a Vehicular Non-Stationary Channel Model," in *6th Int. Symp. Wirel. Veh. Commun.*, no. 1, 2014.

[5] L. Bernadó, N. Czink, T. Zemen, and P. Belanovic, "Physical layer simulation results for IEEE 802.11p using vehicular non-stationary channel model," in *2010 IEEE Int. Conf. Commun. Work.*, May 2010, pp. 1–5.

[6] L. Bernadó, A. Roma, N. Czink, A. Paier, and T. Zemen, "Cluster-based scatterer identification and characterization in vehicular channels," pp. 168–173, 2011.

[7] M. Ester, H. Kriegel, J. Sander, and X. Xu, "A density-based algorithm for discovering clusters in large spatial databases with noise." *Kdd*, 1996.

[8] N. Czink, "The random-cluster model - A stochastic MIMO channel model for broadband communication systems of the 3rd generation and beyond," Ph.D. dissertation, 2007.

[9] N. Czink, T. Zemen, J.-P. Nuutinen, J. Ylitalo, and E. Bonek, "A time-variant MIMO channel model directly parametrised from measurements," *EURASIP J. Wirel. Commun. Netw.*, no. 3, pp. 1–16, 2009.

[10] A. Paier, L. Bernadó, J. Karedal, O. Klemp, and A. Kwoczek, "Overview of vehicle-to-vehicle radio channel measurements for collision avoidance applications," in *2010 IEEE 71st Veh. Technol. Conf.*, 2010, pp. 1–5.